

We are IntechOpen, the world's leading publisher of Open Access books Built by scientists, for scientists

6,900

Open access books available

186,000

International authors and editors

200M

Downloads

Our authors are among the

154

Countries delivered to

TOP 1%

most cited scientists

12.2%

Contributors from top 500 universities



WEB OF SCIENCE™

Selection of our books indexed in the Book Citation Index
in Web of Science™ Core Collection (BKCI)

Interested in publishing with us?
Contact book.department@intechopen.com

Numbers displayed above are based on latest data collected.
For more information visit www.intechopen.com



Structural and Kinematic Analysis of EMS Maglev Trains

Zhao Zhisu

*National University of Defense Technology
China*

1. Introduction

Maglev train is a new means of transport and an integration of the latest high-techs in the field of track-bound transportation system. Over the past half century, the research on vehicle structure has been always a very active area. The researchers realized there is great difference between the movements of the maglev train with that of the conventional rail vehicles. For designing maglev vehicle, creation of a new mechanism is necessary, and then the mechanism is converted to a specific machine to compose vehicles. In this process, machine and mechanism kinematics analysis are indispensable prerequisites. Study of kinematics analysis method and theoretical is the forefront of researching for the structure of maglev train. This chapter aims to introduce author's the latest research outcome.

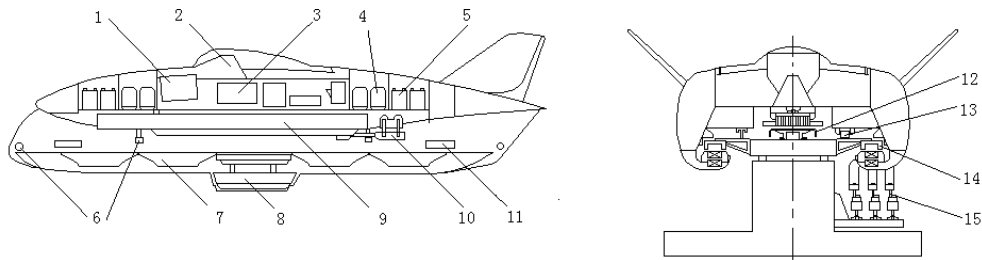
2. Structure of maglev trains

EMS maglev trains have two basic structures which are represented by German Transrapid and Japanese HSST. Chinese and Korean mid-low speed maglev trains are in these two basic structures now.

2.1 Outline of structure development of ems maglev trains

The structure of EMS maglev trains has changed through a rigid aircraft - flexible coupling - modularization structure process. Based on the vehicles levitation running in the air, naturally a structure type of rigid spacecraft has been designed by researchers, namely the whole vehicle in rigid structure. It takes Japanese HSST-01(Yoshio Hikasa & Yutaka Takeuchi, 1980) (Fig.1) and German Transrapid 02(J.L.He et al., 1992) (Fig. 2) as the representatives of this vehicle.

The vehicle shakes violently when they are experimentally running at a high speed. Both kinds of vehicles are non-manned and the researchers design a new kind of maglev vehicle structure for solving the manned riding comfort. This structure separates the car body and running gear first and a secondary suspension system is sets up with buffer spring between them. It takes Japanese HSST-02(Yoshio Hikasa & Yutaka Takeuchi, 1980) (Fig.3) as the representative.

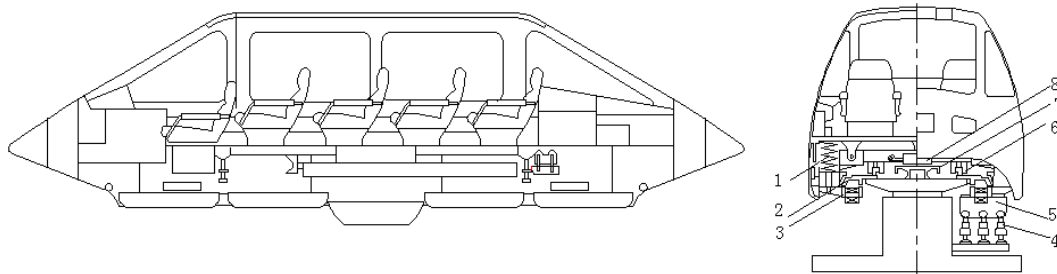


1.Electricity box, 2.Instrument panel, 3.Automate control unit, 4.Thyrist chopper, 5.Battery, 6.Gas sensor, 7.Levitation magnet, 8.Power collector, 9.Linear induction motor, 10.Hydraulic brake, 11.Saving skid, 12.Reaction plate, 13.Brakage, 14.Anchor rail, 15.Power rail

Fig. 1. HSST-01 Maglev Vehicle



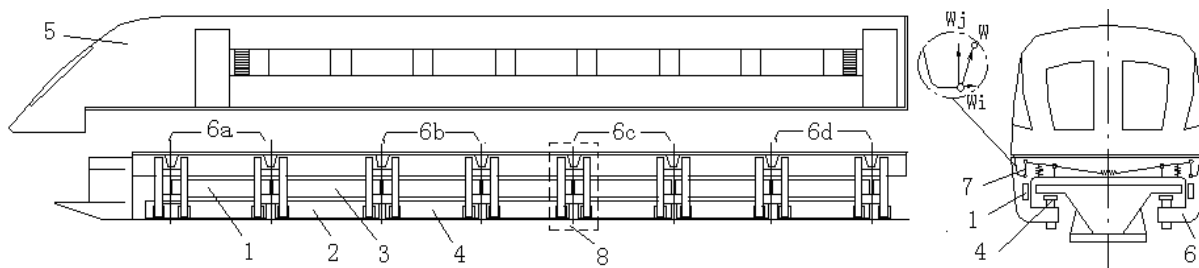
Fig. 2. Transrapid-02



1. Secondary suspend, 2.Anchor rail, 3.Levitation magnet, 4.Power rail, 5.Power collector, 6.Hyraulic brake, 7.Reaction plate, 8.Linear induction motor.

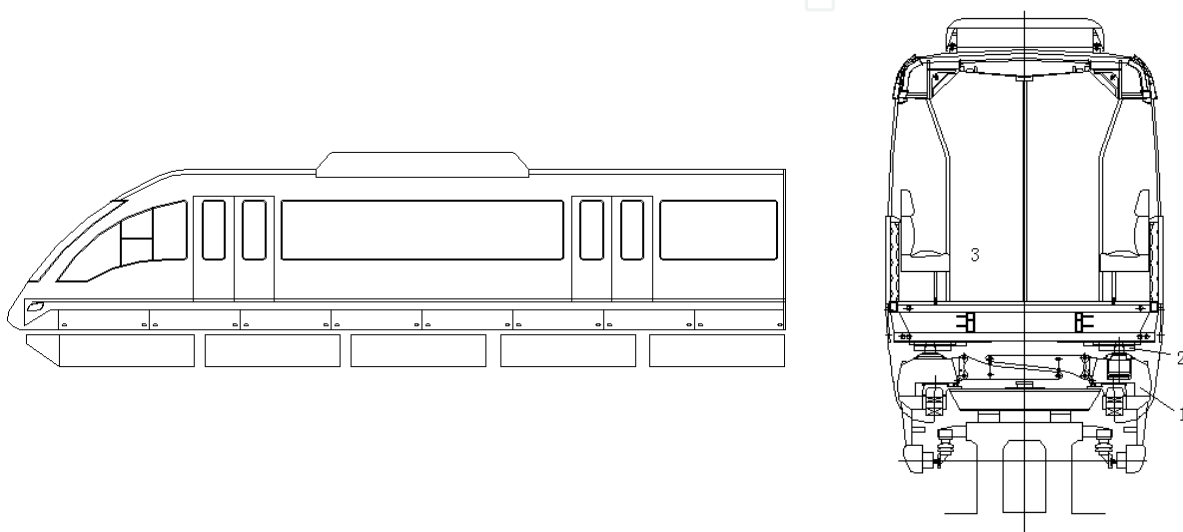
Fig. 3. HSST-02

However, Vibration problem is still unresolved by use of this structure when the train are running at a high speed, because the gap size between magnetic track and suspension electromagnet is acquired by gap sensors which are generally laid for four. The four points should be controlled independently and may not in the same plane (for example, track error, vehicle passing transition curve, asynchronous dynamic adjustment of all points, etc.), but for the rigid or elastic support system in which the bogies are still rigid, the four sensors are installed in a comparatively rigid plane, so this is a conflict. After a long period of experiments and researches, a new kind of modularized vehicle structure (TEJIMA Yuichi, et al., 2004; Seki & Tomohiro, 1995; Maglev Technical Committee, 2007) (Fig.4, 5) is invented. The car body and running gear are separated and jointed by the secondary suspension system in which the four control points of bogies are decoupled, so the vibration problem of vehicles are solved perfectly.



1. Guidance magnet, 2.Overlap magnet, 3.Brake magnet, 4.Levitation magnet, 5.Car body, 6.Maglev bogie, 7.Secondary suspension system, 8.Levitation frame

Fig. 4. Transrapid 08



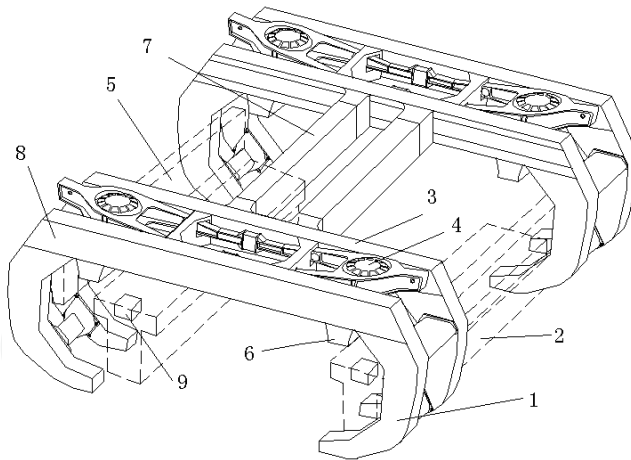
1. Maglev bogie, 2.Secondary Suspend system, 3.Car body.

Fig. 5. HSST-100

2.2 Characteristics of EMS maglev train structure

The structure of maglev trains has several extraordinary characteristics: 1) as light as possible; 2) enough degrees of freedom; 3) special mechanically-braking mode; 4) unique lateral load way 5) vehicles fall on rail to slide under emergency. The vehicles are composed of three parts as shown in Fig.4: car body at the top, secondary suspension at the middle and running gear at the bottom. The wheel rail vehicles have only two bogies through wheel pair contact with rail, but bogies of the maglev trains distributed along the entire length of vehicles, so they are strikingly different in structure.

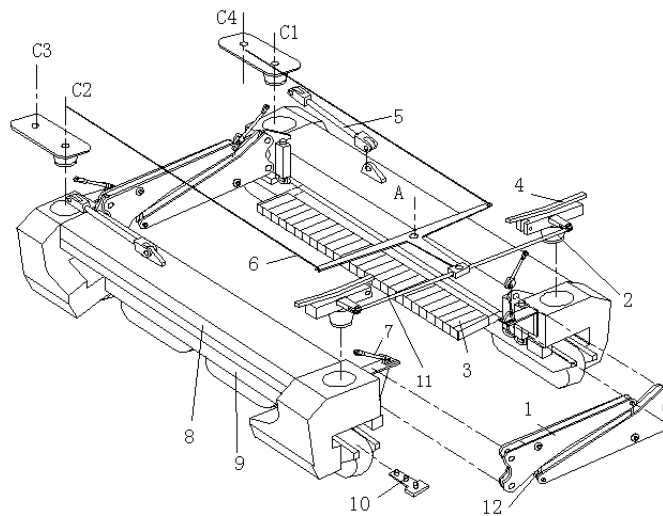
The two wheel pair of wheel rail vehicles is installed on a rigid frame in the same plane. The four points in the frame of maglev bogies, the detection points of gap sensors, should move independently. The bogies have two typical structures: the bogie with torsion longeron is shown as Fig.6 (Maglev Technical Committee, 2007), Fig.8 (Z.S. ZHAO & L.M. YING, 2007). Two levitation frame units 8 are connected by torsion longeron 7 to form The maglev bogies. In vertical direction, the bogies realize the independent motion of four points by reversed longeron (the bogies hereinafter referred as T-type bogies); and the bogie is assembled by connection tow module 8 with anti-rolling beam 1, as shown in Fig.7.



1. Support arm, 2. Levitation magnet, 3. Crossbeam, 4. Air spring & Pendulum arm, 5. Guidance magnet, 6. Support skid, 7. Torsional longeron, 8. Levitation frame unit, 9. Gap sensor

Fig. 6. A bogie of high-speed maglev vehicle

The bogies realize the independent motion of four points by relative torsion of two anti-rolling beams 1 (the bogies hereinafter referred as A-type bogies).



1. Anti-rolling beam, 2. Air spring, 3. Linear induction motor, 4. Linear rolling table, 5. Drive staff, 6. Forced steering mechanism, 7. transverse rod, 8. Module, 9. Levitation magnet, 10. Gap sensor, 11. thrust rod, 12. Rocker.

Fig. 7. A bogie of middle-low speed maglev vehicle

Generally speaking, the running gear of maglev trains is composed of several bogies. The maglev trains and wheel rail trains also differ in the connection among bogies and between bogies and carriages. As shown in Fig.6, bogies are connected by overlap electromagnet 2 and spring hinges to form the maglev running gear (Fig.4), and joints with car body by the tilting suspension system 7. As shown in Fig.7, 9, 10, bogies are grouped in pairs by forced steering mechanisms 6 to make up the running gear, which is connected with the carriages by hinges A · C1~C4 and rolling table 4. The linear rolling table is equipped at the end of bogie modules 8 which can rotate around the shaft C in a small angle. The forced steering mechanism 6 is composed of wire ropes and T-type rod. As it turns, the modules deflect to

drive the air spring transverse rod 7, then the force is transmitted to thrust rod 8 whose motion drives the T-type rod to rotate, the rotation is passed to another T-type rod by linkage wire ropes, then thrust rod and transverse rod of next bogie drive its modules to deflect and so far the steering action is completed.

The secondary suspension system transmits three forces in different directions between car body and bogies and the transmission course is as follows: the vertical load transmits in maglev track \longleftrightarrow electromagnet \longleftrightarrow modules \longleftrightarrow diaphragm air spring \longleftrightarrow rolling table \longleftrightarrow car body.

The transverse load transmits in car body \longleftrightarrow T-type rod \longleftrightarrow wire rope, transverse link \longleftrightarrow lower rolling table \longleftrightarrow air spring tie rod \longleftrightarrow modules \longleftrightarrow electromagnet \longleftrightarrow track.

It can be seen that plenty of bogies distributed along the length of car body contribute to the relative complex joint of car body and bogies. If the tilting suspension system is adopted, the maglev bogie 4 has sixteen pendulum binding mechanisms; if the rolling table is adopted, there are ten point of junction for the steering mechanism.

3. Kinematic characteristics of EMS maglev trains

Although EMS maglev trains fly at a zero height, it still needs exercise along maglev guideway necessary. The position vectors can be divided along guideway (longitudinal), perpendicular guideway surface (vertical), perpendicular guideway side(lateral) three components.

The vertical motion is controlled by the system composed of gap sensor, levitation controller and levitation electromagnet with limitation. The transversal motion is restricted by transversal electromagnetic force and the longitudinal motion is related to the transversal motion and the constraint between all parts of vehicles. According to last paragraph, the vehicle is composed of running gear, secondary suspension system and car body and its kinematic analysis includes the analysis on the spatial positions of all parts and the relative positions of all parts.

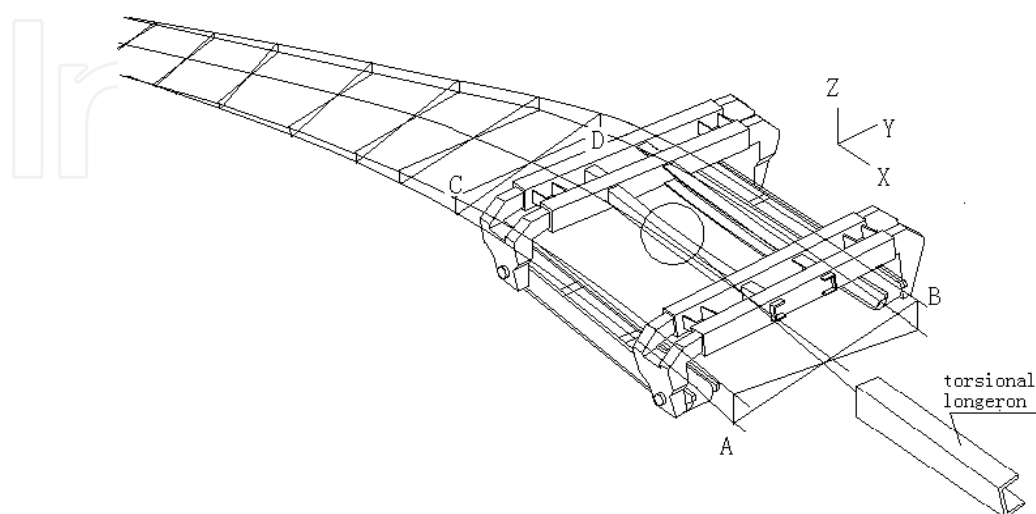
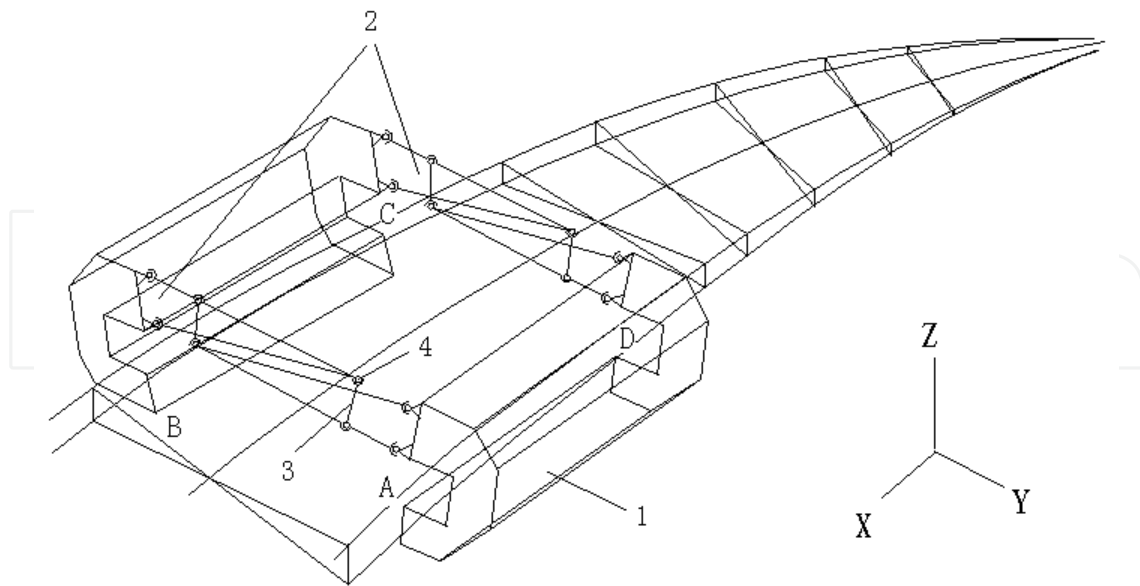


Fig. 8. Bogie Decoupling by torsion beam

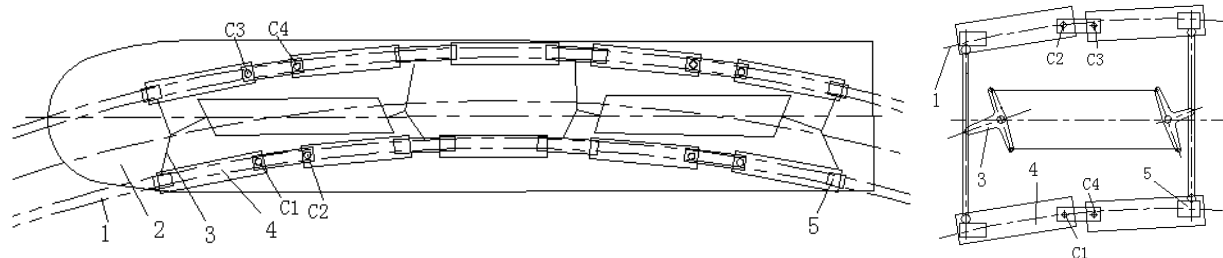


1. Module, 2. anti-rolling beam, 3. pedulum rod, 4. Sphere joint.

Fig. 9. Bogie decoupling by anti-rolling beam

The maglev bogies are the basic components of running gears and their displacements are crucial for the determination of vehicle motion. Their kinematic characteristic is that A, B, C and D points (Fig.8, 9) should move independently (uncoupling). Four straight lines can be drawn by the four points. When the maglev bogies are running along curved path, the four rectilinear motion space surfaces is the Coons surface. When the maglev bogies are passing the transition curve, the four points are not in the same plane. Both A-type bogies and T-type bogies can realize this motion. T-type bogies realize the motion by torsion beams and A-type bogies by the torsion of two anti-rolling beams. However, A-type bogies and T-type bogies have big differences in their transversal motions. The bogie as shown in Fig.6 can only make lateral movement as a whole. In addition, because its secondary suspension system is pendulous and there will produce a big transverse component of gravity force acting on the bogie by pendulum suspension system when the vehicle is passing the curve, the bogie has a bad ability to follow the guideway transversally and can not pass the curve with a small curvature radius and need an active guidance force provided by guidance electromagnet 5 as shown in Fig.6.

Two modules 8 of the bogies as shown in Fig.7 should move independently. Each module has three translational (X, Y, Z) and two rotational (Y, Z) degrees of freedom. It can pass the curves with a small curvature radius and there is hardly any limit in its lateral motion in a small range, so by adopting levitation electromagnet 9 as shown in Fig.6 it can provide a passive guidance force which is a component of levitation force and only exists when the electromagnet is deviating from the guideway and thus it is called as passive guidance force. By now it seems that the motion problem of vehicles has been solved. The track curve can determine the instantaneous position of the bogie, then the relative positions between bogies, bogie and second suspension system and car bodies by connection relationship and the absolute spatial positions of all parts, all of which only involve the deduction of geometric relationships.



1. Railway, 2.Carbody, 3. Forced steering mechanism, 4.Module, 5.Linear bearing.

Fig. 10. Connection between Secondary suspend system, car body & running gear, and two bogies is connected by forced steering mechanism

But the problem is far from simple. For example, the relative position of car body and running gear of vehicle as shown in Fig.4 must be calculated based on the sixteen pendulum suspension mechanisms for the joint of car body and bogie. If the relative position of car body and bogie in the curve changes, the rocker deflects and the weight W of car body transmitted by the sixteen suspenders to the bogie is decomposed into two component forces W_i , W_j , so the transversal relative position of car body and bogie involves the balance of sixteen transversal forces W_i but not a simple calculation of geometric relationships.

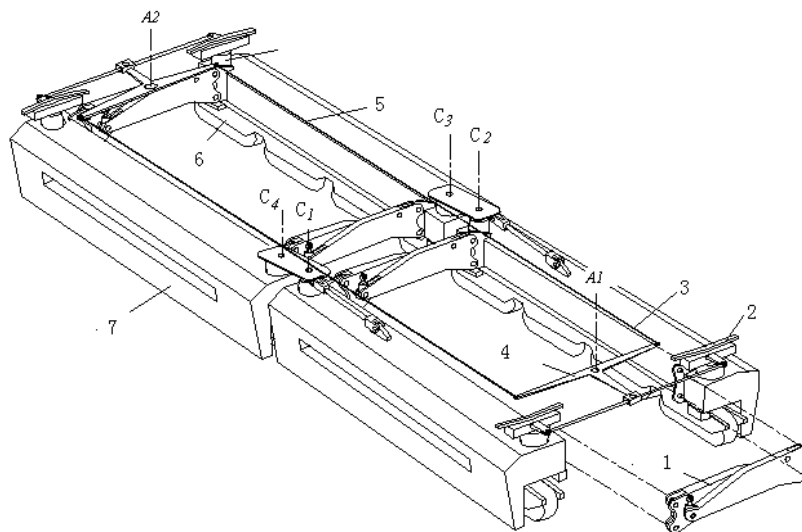
For the vehicle as shown in Fig.5, the constraint of electromagnetic restoring force in the relative position of bogies and track is described in the preceding paragraph. It is easy to calculate the relative position of single bogie and guideway, namely the instantaneous position or locus, then the relative positions or topological relations among all components can be deduced by electromagnetic balance. However, owing to the complexity of connection relationships between several bogies and car body (Fig.10), this calculation method can not be extended to the vehicle. A typical case is when a bogie enters into the transition curve and the following bogie is still in the straight-line guideway, the front bogie rotates around the points C_1 , C_2 and the following bogie is droved to rotate around the points C_3 , C_4 owing to the effect of forced steering mechanism 3, so the following bogie doesn't move along a straight line. The reason lies in that there is a balance relationship of restraining force between the lateral electromagnetic restoring force and components and it should not considered simply that the bogies are pulled to the track by electromagnetic restoring forces. Therefore, different from the wheel rail vehicles, the passive guidance EMS maglev trains may not run in the track curve. The vehicle electromagnetic restoring force, constraint among all components and track geometry curve must be considered comprehensively to deduce the instantaneous position or trace of a bogie in absolute coordinate by the force balance relation and geometrical relation of vehicle in any position, then the relative positions between the rigid bodies or topological relations of all components are deduced by connection relations. However, it brings big difficulties in solving this problem.

4. Kinematic modeling and analysis of maglev trains (Z.S. Zhao and C. Ren, 2009)

The kinematic characteristics of EMS maglev trains illustrated in the preceding paragraph show that the motion of maglev trains can not be deduced simply by geometrical relations. Based on the passive EMS maglev trains, the following kinematic analysis includes

kinematic modelling and analysis. The vertical position of vehicle is controlled by the levitation gap between electromagnet and guideway. Because the gap is constant, the vertical position of vehicle can be determined by the track curve and the determination of lateral instantaneous position is the key of kinematic research on vehicles.

The research on instantaneous position adopts two methods based on track fitting: strict fitting track (two endpoints of the bogie on the track) (ZHAO Z.S. & YING L.M., 2000; MEI Z. & LI J., 2007; JIANG H.B., et al., 2007) and balanced lateral electromagnetic restoring force of single bogie (ZENG Y.W. & WANG S.H. 2003; ZHANG K. & LI J., 2005; ZHAO C.F & ZAI W.M., 2005). The former is obviously an unproved hypothesis and the later doesn't consider the influence of constraint among all components in the motion.



1. Anti-rolling beam, 2. Linear rolling table, 3. forced steering mechanism, 4. T type rod, 5. Wire rope, 6. Levitation magnet, 7. module.

Fig. 11. Running gear sketch of the passiveness guidance EMS maglev train

4.1 Kinematic modelling of EMS mid-low speed maglev trains

To simplify the problem without loss of generality, in this article derivations is made based on the following conditions: 1) because the Z-directional motion of vehicle has a little influence on its lateral motion, its mathematical deduction is based on X-Y plane; 2) the model is established for the vehicle with four bogies; 3) the axis C_1 - C_4 are combined into two axis P_4 , P_{11} (Fig.12); 4) the kinematic modelling is only based on the central line of track; 5) the carriages and bogies are rigid bodies with the lengths of L_C 、 L respectively.

4.1.1 Kinematic modeling of maglev trains based on geometrical relations

In the instantaneous position sketch of maglev trains as shown in Fig. 12, $P_i (x_i, y_i)$ represent bogies' end point and intersection point of bogies and track curve $Y(x)$. If P_i is definite, the instantaneous position or motion locus of vehicle and the relative positions (topological relations) among the components of vehicle and between vehicle and track may be determined. The section aims to establish the equations with the unknown quantities x_i, y_i

accordingly based on geometrical relations. P_i is in the straight line representing bogies respectively and should satisfy the following relations:

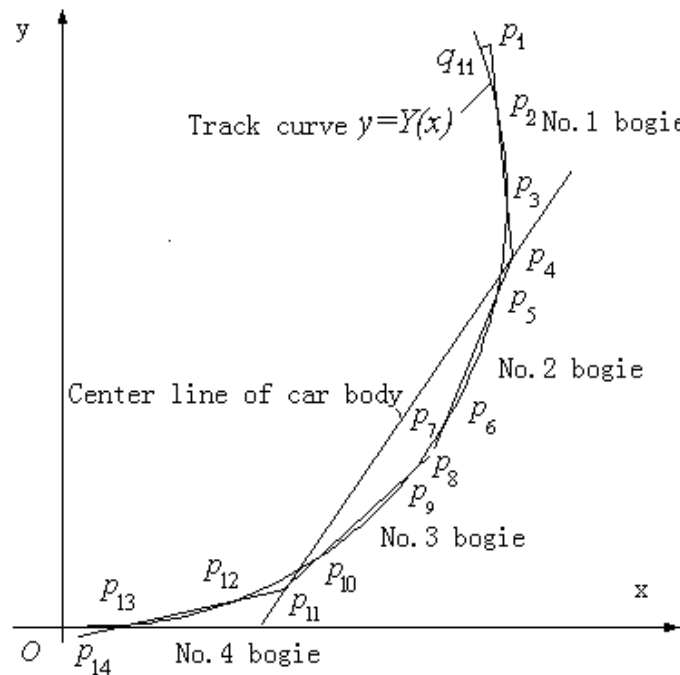


Fig. 12. Instantaneous Position of the maglev vehicle with four bogies

$$\left. \begin{aligned} \frac{(y_i - y_{i+2})}{(x_i - x_{i+2})} - \frac{(y_{i+1} - y_{i+2})}{(x_{i+1} - x_{i+2})} &= 0 \\ \frac{(y_{i+3} - y_{i+1})}{(x_{i+3} - x_{i+1})} - \frac{(y_{i+2} - y_{i+1})}{(x_{i+2} - x_{i+1})} &= 0 \\ (x_i - x_{i+3})^2 + (y_i - y_{i+3})^2 &= L^2 \end{aligned} \right\} \quad (4-1)$$

There $i=1, 4, 8, 11$. The geometrical relation between carriage and bogie is:

$$\sqrt{(x_4 - x_{11})^2 + (y_4 - y_{11})^2} = 0.5L_c \quad (4-2)$$

The intersection relation of curve and straight line is:

$$\left. \begin{aligned} \frac{y_i - Y(x_{i+2})}{x_i - x_{i+2}} - \frac{Y(x_{i+1}) - Y(x_{i+2})}{x_{i+1} - x_{i+2}} &= 0 \\ \frac{y_{i+3} - Y(x_{i+1})}{x_i - x_{i+1}} - \frac{Y(x_{i+2}) - Y(x_{i+1})}{x_{i+2} - x_{i+1}} &= 0 \end{aligned} \right\} \quad (4-3)$$

In the above equation, $i=1, 4, 8, 11$. The straight line representing the centre line of carriage is:

$$\left(\frac{y_4 - y_{11}}{x_4 - x_{11}} \right) x - y - \left(\frac{y_4 - y_{11}}{x_4 - x_{11}} \right) x_4 + y_4 = 0$$

The offset distance from the bogie endpoints to the car body obtained by the distance from point to line: $\Delta_i = \frac{(y_4 - y_{11})(x_i - x_4) - (x_4 - x_{11})(y_i - y_4)}{0.5L_c}$, in which $i=1,7,8,1$. Follow equation

(ZHAO Z.S. et al., 2000) is given by the structural symmetry and the constraint of forced steering mechanism,

$$\frac{\Delta_1}{\Delta_7} = \frac{\Delta_{14}}{\Delta_8} \quad (4-4)$$

there are twenty-two equations with twenty-eight unknown quantities $P_i(x_i, y_i)$ in the above (4-1)-(4-4), it is obvious that the kinematic problem of vehicle can not be solved only by geometrical relations and other equations should be founded by the balance relations of lateral forces.

4.1.2 Kinematic modeling of maglev trains based on the constraint of lateral electromagnetic restoring force and mechanism constrain

The passive guidance EMS maglev train keeps a lateral position from electromagnetic restoring force. To seek balance of lateral force, it should be considered that the calculation of electromagnetic resilience generated by the linear bogie units fitting the curved track; the influence of constraint such as the binding force produced among the bogies owing to interconnection of the forced steering mechanisms and carriages and bogies. In this section, other equations shall be sought for by the balance of lateral forces, the calculation formula of lateral forces (Sinha P. K., 1987) is:

$$F_u = K_m L_w \tan^{-1} \left(\frac{\Delta u}{\delta} \right)$$

in which $K_m = \frac{\mu_0 N^2 I^2}{4\pi\delta}$, $L_w = \frac{A}{W_m}$, L_w is length of magnetic pole, μ_0 , N , A , I represents

vacuum permeability and turns, effective area of magnetic pole, coil current respectively, other parameters can refer to Fig.13. Taking the first bogie for example, the electromagnetic restoring force of any infinitesimal curve unit d_s in the track is:

$$dF_{u1} = K_m \tan^{-1} \left(\frac{\Delta u_1}{\delta} \right) dL_w$$

Δu_1 represents the distance from a point $q(x, y)$ in the curve to the line:

$$\Delta u_1 = \frac{(y_1 - y_4)x - (x_1 - x_4)y + x_1 y_4 - x_4 y_1}{L}, \text{ seeing to (Fig. 13), } dL_w = \cos(\alpha_s - \alpha_1) ds,$$

$ds \cos \alpha_s = dx$, $k_s = \tan \alpha_s$, $k_1 = \tan \alpha_1 = \frac{y_1 - y_4}{x_1 - x_4}$, dF_{u1} can be written as :

$$dF_{u1} = \frac{1 + k_s k_1}{\sqrt{1 + k_1^2}} K_m \tan^{-1} \left(\frac{\Delta u_1}{\delta} \right) dx$$

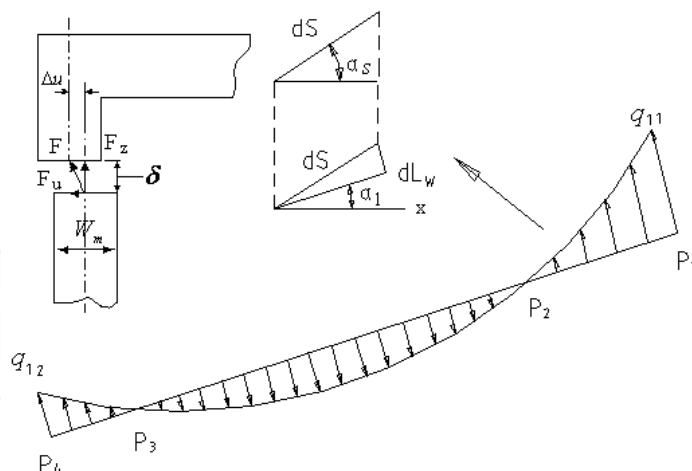


Fig. 13. Magnet lateral reversion force of the bogie module

In the same way, the calculation formula of the electro magnetic restoring force differential unit of other bogies can be deduced:

$$F_{ui} = \int_{x_{i1}}^{x_{i2}} K_m \frac{1 + k_s k_i}{\sqrt{1 + k_i^2}} \tan^{-1} \left(\frac{\Delta u_i}{\delta} \right) dx \quad (i=1,2,3,4) .$$

1. Balance equation of lateral restoring force and moment of the vehicle:

$$\left. \begin{aligned} \sum F_x &= \sum_i F_{ui} \sin \alpha_i = 0 \\ \sum F_y &= \sum_i F_{ui} \cos \alpha_i = 0 \end{aligned} \right\}$$

$$\left. \begin{aligned} \sum_i \int_{x_{i1}}^{x_{i2}} K_m \frac{(1 + k_s k_i) k_i}{1 + k_i^2} \tan^{-1} \left(\frac{\Delta u_i}{\delta} \right) dx &= 0 \\ \sum_i \int_{x_{i1}}^{x_{i2}} K_m \frac{1 + k_s k_i}{1 + k_i^2} \tan^{-1} \left(\frac{\Delta u_i}{\delta} \right) dx &= 0 \end{aligned} \right\} \quad (4-5)$$

Balance equation of moment of lateral restoring force (taking P₄ as the pivoting point)

$$\left. \begin{aligned} \sum_{i \neq 3} \int_{x_{i2}}^{x_{i1}} K_m \frac{1 + k_s k_i}{1 + k_i^2} \tan^{-1} \left(\frac{\Delta u_i}{\delta} \right) (-1)^i (x_4 - x) dx + \\ + \int_{x_{32}}^{x_{31}} K_m \frac{1 + k_s k_3}{1 + k_3^2} \tan^{-1} \left(\frac{\Delta u_i}{\delta} \right) (x - x_4) dx &= 0 \\ \sum_{i \neq 3} \int_{x_{i2}}^{x_{i1}} K_m \frac{(1 + k_s k_i) k_i}{1 + k_i^2} \tan^{-1} \left(\frac{\Delta u_i}{\delta} \right) (-1)^i (y_4 - Y(x)) dx + \\ + \int_{x_{32}}^{x_{31}} K_m \frac{(1 + k_s k_i) k_3}{1 + k_3^2} \tan^{-1} \left(\frac{\Delta u_i}{\delta} \right) (Y(x) - y_4) dx &= 0 \end{aligned} \right\} \quad (4-6)$$

2. Balance of constraint force of forced steering mechanism

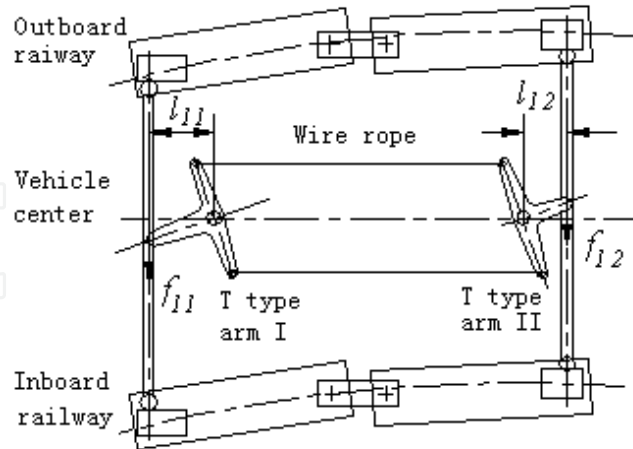


Fig. 14. Balance of two bogies linked by compelling guided mechanism

3. According to Fig.14, the balance equation of constraint force of forced steering mechanism linking the No.1,2 bogies is $f_{11}l_{11}=f_{12}l_{12}$, and the following equation can be obtained:

$$f_{12} = f_{11} \frac{l_{11}}{l_{12}} = \eta f_{11} \tag{4-7}$$

The moment arm length from the point P_4 to No.1 bogie's any point dFu_1 on which electromagnetic resilience is exerted is $\frac{x-x_4}{\cos\alpha_1} = (x-x_4)\sqrt{1+k_1^2}$, the balance relation of No.1

bogie module's moment is $0.5f_{11}L\cos\alpha_1 = \int_{x_{11}}^{x_{12}} K_m(1+k_s k_1)(x-x_4)\tan^{-1}\left(\frac{\Delta u_1}{\delta}\right)dx$, namely,

$f_{11} = \frac{2}{L} \int_{x_{11}}^{x_{12}} K_m(1+k_s k_1)\sqrt{1+k_1^2}(x-x_4)\tan^{-1}\left(\frac{\Delta u_1}{\delta}\right)dx$, similarly f_{12} can be obtained, and substituted in (7) :

$$\sum_{i=1,2} \eta^{2-i} \int_{x_{i2}}^{x_{i1}} K_m(1+k_s k_i)\sqrt{1+k_i^2}(x_4-x)\tan^{-1}\left(\frac{\Delta u_i}{\delta}\right)dx = 0 \tag{4-8}$$

By the above method the constraint forces' balance equation of forced steering mechanisms connecting No.3, 4 bogies can be obtained:

$$\sum_{i=3,4} \eta^{i-3} \int_{x_{i2}}^{x_{i1}} K_m(1+k_s k_i)\sqrt{1+k_i^2}(x-x_{11})\tan^{-1}\left(\frac{\Delta u_i}{\delta}\right)dx = 0 \tag{4-9}$$

The upper or lower limit of integration are the coordinate x of the intersection points q_{i1} 、 q_{i2} of two straight lines perpendicular to the endpoints P_i 、 P_{i+3} of the No.1 bogie and the curve $Y(x)$. Its expression is written as (corresponding to four bogies, $j=1, 4, 8,$ and 11):

$$\left. \begin{aligned} k_i(x_{i1} - x_j) + (Y(x_{i1}) - y_j) &= 0 \\ k_i(x_{i2} - x_{j+3}) + (Y(x_{i2}) - y_{j+3}) &= 0 \end{aligned} \right\}$$

Substituting $x_{11} \cdot y_{11} = Y(x_{11})$ in the above first equation, the following equation can be obtained:

$$k_1(x_{11} - x_1) + (Y(x_{11}) - y_1) = 0 \quad (4-10)$$

In the above six equations in (4-5) (4-6) (4-8) (4-9) obtained by the balance between lateral electromagnetic resilience and structural constraint force, the equations (8), (9) introduce a unknown quantity η . Hereby the equation (4-10) is introduced and a reference point $q_{11} (x_{11} \cdot y_{11})$ to instantaneous position of vehicle is given. The equations (4-1)-(4-6) and (4-8)-(4-10) are the non-linear equation set with twenty-nine unknown quantities, namely twenty-nine unknown quantities $P_i (x_i \cdot y_i)$ and η can be resolved. This is the general formula for kinematic analysis on passive EMS maglev trains with four bogies which can be used to resolve the absolute position (motion trace) of any bogie and the relative position or topological relation of any component of the vehicle at any time. In the same way, kinematics equations of maglev train with other number bogies can be deduced.

4.1.3 General kinematic characters of passive guidance EMS maglev trains

Following kinematic characters of vehicles can be deduced by the above general kinematic formulas:

Character 1: kinematic the static determinacy or indeterminacy of vehicles is determined by the forced steering mechanism, namely the topological relation between a bogie and carriage (formula (4-4), (4-7)) must be given and if not, there will be multiple solutions of motion trace.

Character 2: n , namely the number of intersection points of the modules (straight line) and track (convex curve), $1 \leq n \leq 2$, two geometric equations will be reduced for each reduced crossing point and in the straight-line segment of track, the bogies are coincident with the track.

Character 3: the motion trace of vehicle is determined together by the topological relations between bogie and carriage and bogie and track but not only by the track.

Character 4: The steering characteristic and yawing characteristic of vehicle with transverse interference depend on the balance relation between the lateral electromagnetic restoring force and the constraint force of forced steering mechanism.

4.2 Solution and analysis of kinematic equations of EMS mid-low speed maglev trains

Given that $N=320$, $W_m=28$ mm, $A=3360 \times 28$ mm², $L=3.4$ m, $L_c=14.5$ m, circular curve radius $R=100$ m, superelevation is 60 mm, transition curve length $l_0=12$ m, the easement trace curve is the clothoid generally, the curvature of easement curve $k = s \div Rl_0$ and the high-order small quantities are ignored, the projection of x-y plane of trace curve is:

$$y=Y(x) = \begin{cases} 0 & x \leq 0 \\ \frac{x^3}{6l_0R} & 0 < x < x_e \\ y_c - \sqrt{R^2 - (x-x_c)^2} & x_e \leq x \end{cases}$$

in which $q_0(x_0, y_0)$, $q_e(x_e, y_e)$, $q_c(x_c, y_c)$ represent the bonding points of the straight segment and curved segment of trace curve $Q(x)$ and transition curve and the center of bend circular curve respectively. $x_c = x_e - \frac{k_e R}{\sqrt{1+k_e^2}}$, $y_c = y_e + \frac{k_e R}{\sqrt{1+k_e^2}}$, $k_e = Y'(x)|_{x=x_e}$, $q_e(11.9956, 0.2397)$, $q_c(11.6364, 100.06)$. In the interval defined by track curve, a series of $q_{11}(x_{11}, y_{11})$ are valued according to the step length of 0.1m to resolve the kinematic equations obtained in the preceding paragraph, the motion trace of vehicle and the relative positions of all vehicle components can be derived. Some primary results obtained through numerical calculation by MATHEMATICA are given below.

1. Motion trace

To express the kinematic characters, the motion trace of vehicle is shown by the offset of bogies to the track but not the coordinate figure P_i . The fig.15 gives the fitting figure of computed results and the table 1 shows the computed results when q_{11} is valued as four typical coordinate points.

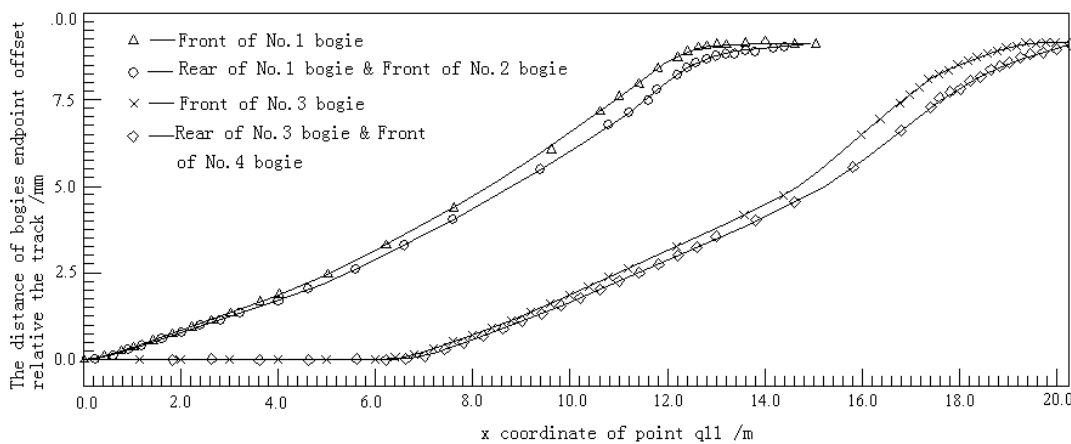


Fig. 15. Curves of bogies endpoint offset relative to the track

Bogie $q_{11}(x,y)$	1		2		3		4	
	Front Δu_{11}	Rear Δu_{12}	Front Δu_{21}	Rear Δu_{22}	Front Δu_{31}	Rear Δu_{32}	Front Δu_{41}	Rear Δu_{42}
3.4, 0.0055	1.94	1.89	1.89	1.91	0	0	0	0
6.8, 0.0437	3.52	3.49	3.49	3.5	0	0	0	0
10.2, 0.1474	6.52	6.46	6.46	6.48	1.91	1.89	1.89	1.92
13.6, 0.3494	8.05	7.94	7.94	8.01	3.52	3.51	3.51	3.53

Table 1. Δu_{ij} , Amount of bogie endpoint offset relative to the track

2. Relative positions of all components of vehicle

The relationships of relative positions exist among the bogies and between bogies and carriages. For the sake of intuition, the computed results of relative positions among bogies are transformed into the included angles. The figure 16 gives the fitting figure of computed results of relative positions among bogies and the Tab. 2 gives the computed results of two position relations when q_{11} is valued as four typical coordinate points respectively

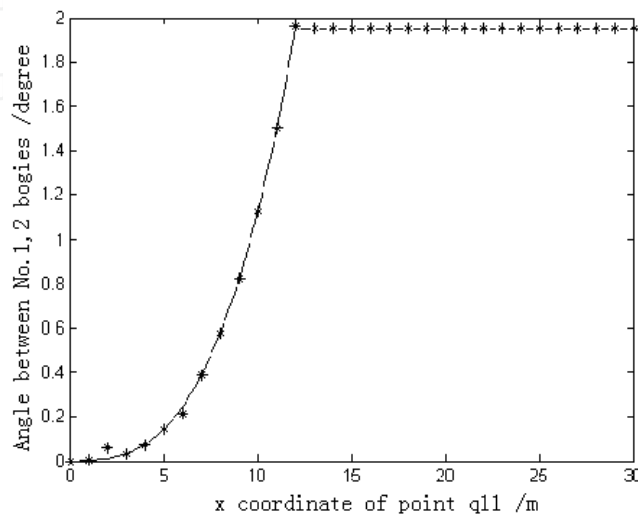


Fig. 16. Alteration curve of angle between No.1,2 bogies

Bogie P11(x,y)	1	2	3	4	1-2	2-3	3-4
	Front Δ_1	Rear Δ_7	Front Δ_8	Rear Δ_{14}	θ_{12}	θ_{23}	θ_{34}
3.4, 0.0055	3.24	1.05	0.84	0.84	0.034°	0.02°	0°
6.8, 0.0437	13.78	4.52	1.02	1.02	0.424°	0.215°	0°
10.2, 0.1474	95.75	31.81	27.24	83.92	1.072°	0.556°	0.039°
13.6, 0.3494	157.8	52.54	48.05	146.03	1.771°	1.091°	0.411°

Table 2. Angle θ_{ij} between bogies & Bogie endpoint offset Δ_i relative to the car body

4.3 Conclusions

Based on the derivation and computational analysis of above kinematic mathematical formulas and test results, the following conclusions on relevant kinematic researches on passive guidance EMS maglev trains can be obtained.

1. The absolute position or trace of vehicle is not equal to track curve and their relation (offset Δ_{ij}) is also not constant. The change rule is: straight segment (zero) → easement curve segment (Monotone increasing) → bend segment (a maximum constant)
2. The kinematic static determinacy or indeterminacy of vehicles depends on the forced steering mechanism. If no forced steering mechanism, the kinematic relation of vehicles is indefinite.
3. The bogie and carriage, bogie between any two are restricted geometrically and the bogie and track is constrained by lateral electromagnetic restoring force, so the absolute

position Δu_{ij} of bogies should be determined by the electromagnetic balance of vehicle and geometrical constraint relations of all its components. Δu_{ij} of different bogies is different at the same time and position.

4. The parameter $\eta=3$ expressing the characteristic of relative position between bogies and carriages is applicable to all line segments.
5. The change law of relative position (θ_{ij}) among bogies is: straight segment (zero) \rightarrow easement curve segment (Monotone increasing) \rightarrow bend segment (a maximum constant).
6. The absolute position of vehicle and the relative position among all its components including the bonding points of all line segments change smoothly in the motion.
7. The results obtained by kinematics formulas are consistent with the past research results in circular curve and straight-line segment
8. The article gives that the mathematical models can be used in the kinematic analysis of vehicle by the transverse interference.

5. Kinematic analysis on the secondary suspension system of maglev trains

The composition and kinematic characteristics of secondary suspension system for the joint of car body and bogies has been illustrated in the paragraph 1, 2. The distinctive mid-structure of active and passive guidance maglev trains lie in pendular suspension mechanism and forced steering mechanism respectively. In this paragraph, their kinematic characteristics analysis and the calculation method is given and other kinematic analyses can see the references (ZHAO Z.S. et al., 2000).

5.1 Kinematic analysis on the forced steering mechanism of passive guidance ems maglev trains

The functions of forced steering mechanism are to connect two bogies to form the running gear (Fig.10, 11, 14), keep a proper geometric position between the running gear and car body (Fig.10) and transmit the transversal force between the running gear and car body. When realizing these functions, the uncoupling of bogies can not be affected by the mechanism. According to Fig.14, the transverse thrust rod of the forced steering mechanism may affect the uncoupling of bogies, which can be obtained by analyzing some motions of bogie as it goes through the curve.

The relative height and distance between the ends of two bogie modules in motion may change. The transverse thrust rod are equipped at the end of bogies, so it is possible to add spherical hinges at the end of links to adapt to the change of relative height between the ends of two modules and it is hard to change the length of rigid rods. Take the vehicle with five bogies Shown as Fig.17 for example. Setting : $\delta_1=\alpha_2-\alpha_1$, $\delta_2=\varphi_2-\varphi_1$, h , β , L represent width of track and angle of a $\cdot R_2$, length of module respectively.

$$\phi_i = \sin^{-1}\left(\frac{L}{2R_i}\right) , \quad \alpha_i = 5\phi_i ,$$

outside track radius is $R_1 = R+h/2$, inside track radius is $R_2 = R-h/2$, distance between two module endpoints of bogie in the curve : $a_i = \sqrt{R_1^2 + R_2^2 - 2R_1R_2 \cos \delta_i}$, there $i=1,2$.

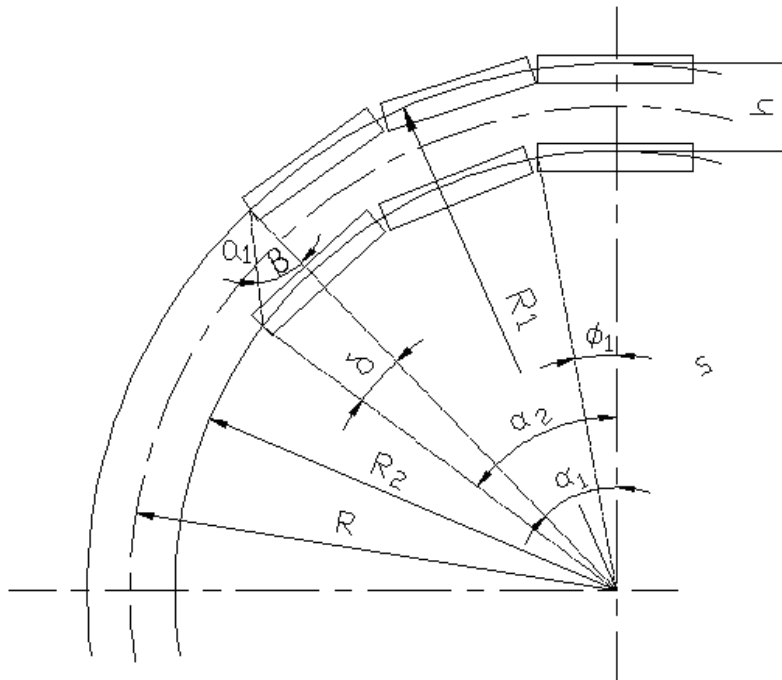


Fig. 17. Distance between two module endpoints of bogie in a curve

Obviously the distance between two module endpoints of bogie in a curve is enlarged relatively to in straight. Its size can be examined by an instance.

Given that $R=50\text{m}$, $h=2.02\text{m}$, $L=2.24\text{m}$

$$\varphi_1=1.25811$$

$$\varphi_2=1.31$$

The distance between two module endpoints of front bogie is:

$$a_1 = \sqrt{48.99^2 + 51.01^2 - 2 \times 48.99 \times 51.01 \times \cos(0.2594)} = 2.03264\text{m}$$

The distance between two endpoints of back bogie : $a_2=2.0205\text{m}$, a_1 , a_2 represents the distance between endpoints of front and back bogies in a curve respectively, and the change of distance between two module endpoints of bogie is:

$$D_{a1}=a_1-h=12.64\text{mm}$$

$$D_{a2}=a_2-h=0.5\text{mm}$$

Therefore, the change of distance between two module endpoints of front bogie is bigger and transverse thrust rod must be able to extend 13mm at most when the vehicle is in motion. To solve this problem, the transverse thrust rod may be arranged in a V type (Fig.18) and the calculation of physical dimension of the forced steering mechanisms and their mathematical models based on kinematics principle is given below.

As shown in Fig.17, L 、 t 、 l 、 d 、 f represent length of module and transverse thrust rod and T-type arm, the horizontal distances from rotation center of module to rotation centre of T-type rod, the offset distance between the hinge point of transverse thrust rod and the center of air spring respectively. θ_1 , θ_2 represent the oscillation angle of two modules respectively.

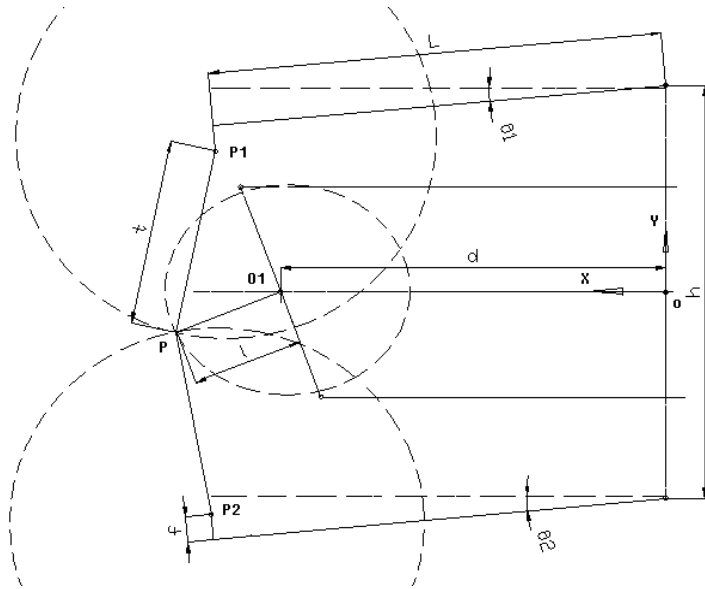


Fig. 18. Kinematic sketch of forced steering mechanism

When the running gear is in motion, two transverse thrust rod and T-type rod rotate around the point $P_1(x_1, y_1)$, $P_2(x_2, y_2)$ and O_1 respectively and the traces of their endpoints are three circles in the same plane with the radius of t , 1 . Three circles intersect in the point $P(x, y)$. Thereout the following equation set is given.

$$\left. \begin{aligned} (x - x_1)^2 + (y - y_1)^2 &= t^2 \\ (x - x_2)^2 + (y - y_2)^2 &= t^2 \\ (x - d)^2 + y^2 &= l^2 \end{aligned} \right\} \tag{5-1}$$

among which,

$$\left. \begin{aligned} x_i &= L \cos 4\alpha_i + (-1)^i f \sin 4\alpha_i \approx L \sqrt{1 - \frac{4L^2}{R_i^2}} \\ y_i &= (-1)^{i-1} (h - f \cos 4\alpha_i) - L \sin 4\alpha_i \approx (-1)^{i-1} (h - f) - \frac{2L^2}{R_i} \end{aligned} \right\} \tag{5-2}$$

In the above equation set, $i=1, 2$, and by the third equation in (1), $y = \sqrt{l^2 - (x - d)^2}$ is obtained.

In consideration of $x_1 \approx x_2$, by the first and second equations in (1), $y = -L^2 \left(\frac{1}{R_1} + \frac{1}{R_2} \right)$ is obtained and is substituted into second equations in (5-1) :

$x_2 + \sqrt{t^2 - [h - f + L^2 \left(\frac{1}{R_2} - \frac{1}{R_1} \right)]^2} = x$, thus the x, y is obtained and substituted respectively into third equation in (5-1):

$$\left(\sqrt{t^2 - \left[h - f + L^2 \left(\frac{1}{R_2} - \frac{1}{R_1}\right)\right]^2 + L - d}\right)^2 + L^4 \left(\frac{1}{R_1} + \frac{1}{R_2}\right)^2 = l^2 \quad (5-3)$$

Without considering of high-order small quantities, the equation (3) can be simplified as:

$$\left(\sqrt{t^2 - (h - f)^2} + L - d\right)^2 = l^2 \quad \text{or} \quad t^2 = (l + d - L)^2 + (h - f)^2$$

There are two unknown quantities t and l in the above equation. One of them is set, the other can be obtained. A calculation sample is given below.

Given that $L=2.24\text{m}$, $h=2\text{m}$, $R=50\text{m}$, $f=90\text{mm}$, $d=1.9\text{m}$ and $l=550\text{mm}$, $t \approx 1.39\text{m}$ can be obtained.

5.2 Kinematic analysis on tilting suspension system of maglev train

5.2.1. Mathematical description of turing characteristic of tilting suspension system maglev train (Zhao Z.S., 2009)

The figure 18 show the motion state of high-speed maglev train with tilting suspension system goes around the curve, in which Δ_{ij} , θ_{ij} represent the lateral displacement and oscillation angle of rocker respectively and w 、 T_{ij} 、 f_{ij} represent the car body gravity, tension and lateral force of carriage acting on the rockers of tilting suspension system respectively. The train is composed of carriage, bogies, suspension system. four bogies and three overlapping modules are connected alternately to form the running gear (see the Fig. 18 left) and four set of pendular suspension systems are configured in the interval between four bogies and carriage respectively (see the Fig. 18 right). As the vehicle enters the curve, the bogies move along the track curve under the effect of active electromagnetic guiding force and produce relative displacement Δ_{ij} to the carriage which is driven by the oscillation of rockers of tilting suspension system. The sixteen pendular rod of tilting suspension system will produce the lateral force acting on the carriage and bogies. Δ_{ij} is determined by the balance of the forces f_{ij} acting on the carriage, the active electromagnetic guiding force can be obtained by the force f_{ij} acting on single bogie. Therefore the solution of the steering characteristic of maglev train with tilting suspension system lies in resolving the displacement of rockers and the force acting on them. From the viewpoint of design, it might as well make a hypothesis that the sixteen rockers receive the weight of carriage equally.

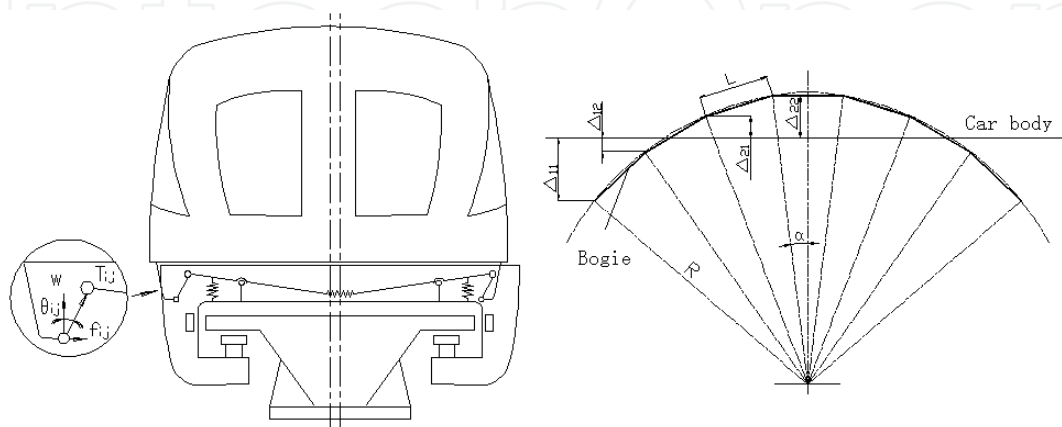


Fig. 19. Force and Displacement of Tilting Suspension System & Relative Displacement between Carriage and Bogie in the Curve

The lateral balance equation of carriage in the curve is:

$$\sum_{i=1}^4 \sum_{j=1}^2 \vec{f}_{ij} = 0 \text{ , because of the symmetry, } 2 \sum_{i=1}^2 \sum_{j=1}^2 \vec{f}_{ij} = 0 \text{ ,}$$

in the above equations, the bilateral balances are considered similarly and $i \cdot j$ represent the number of bogie and its ends respectively. The above equation can be written as:

$$w(\tan \theta_{11} + \tan \theta_{12} - \tan \theta_{21} - \tan \theta_{22}) = 0 \quad (5-4)$$

namely:

$$\frac{\Delta_{11}}{\sqrt{l^2 - \Delta_{11}^2}} + \frac{\Delta_{12}}{\sqrt{l^2 - \Delta_{12}^2}} = \frac{\Delta_{21}}{\sqrt{l^2 - \Delta_{21}^2}} + \frac{\Delta_{22}}{\sqrt{l^2 - \Delta_{22}^2}} \quad (5-5)$$

among which l represent the length of rocker. The following geometrical relationships can be shown in Fig. 18:

$$\Delta_{11} = \Delta_{12} + L \sin 6\alpha$$

$$\Delta_{22} = \Delta_{21} + L \sin 2\alpha$$

Substituted into (2):

$$\frac{\Delta_{12} + L \sin 6\alpha}{\sqrt{l^2 - (\Delta_{12} + L \sin 6\alpha)^2}} + \frac{\Delta_{12}}{\sqrt{l^2 - \Delta_{12}^2}} = \frac{\Delta_{21}}{\sqrt{l^2 - \Delta_{21}^2}} + \frac{\Delta_{21} + L \sin 2\alpha}{\sqrt{l^2 - (\Delta_{21} + L \sin 2\alpha)^2}} \quad (5-6)$$

Likewise from the geometrical relationships, the following equation can be obtained:

$$\Delta_{12} + \Delta_{21} = L \sin 4\alpha \quad (5-7)$$

From trigonometric functional relations and in considering of $R \gg L$:

$$\sin 2\alpha = 2 \sin \alpha \cos \alpha = \frac{L}{2R} \sqrt{1 - \left(\frac{L}{2R}\right)^2} \approx \frac{L}{2R}$$

$$\sin 4\alpha = 4 \sin \alpha \cos^3 \alpha = \frac{2L}{R} \left(1 - \left(\frac{L}{2R}\right)^2\right)^{\frac{3}{2}} \approx \frac{2L}{R}$$

$$\sin 6\alpha = 2(3 \sin \alpha - 4 \sin^3 \alpha)(4 \cos^3 \alpha - 3 \cos \alpha) = \frac{L}{R} \left(3 - \left(\frac{L}{R}\right)^2\right) \left(1 - \left(\frac{L}{R}\right)^2\right) \sqrt{1 - \left(\frac{L}{2R}\right)^2} \approx \frac{3L}{R}$$

From the above three equations, given that $m=L^2/R$ and substituted in (3), (4) :

$$\left. \begin{aligned} \frac{\Delta_{12} + 3m}{\sqrt{l^2 - (\Delta_{12} + 3m)^2}} + \frac{\Delta_{12}}{\sqrt{l^2 - \Delta_{12}^2}} &= \frac{\Delta_{21}}{\sqrt{l^2 - \Delta_{21}^2}} + \frac{\Delta_{21} + 0.5m}{\sqrt{l^2 - (\Delta_{21} + 0.5m)^2}} \\ \Delta_{12} + \Delta_{21} &= 2m \end{aligned} \right\} \quad (5-8)$$

among which L represent the length of bogie. From the equations (5),

$$\frac{5m - \Delta_{21}}{\sqrt{l^2 - (5m - \Delta_{21})^2}} + \frac{2m - \Delta_{21}}{\sqrt{l^2 - (2m - \Delta_{21})^2}} = \frac{\Delta_{21}}{\sqrt{l^2 - \Delta_{21}^2}} + \frac{\Delta_{21} + 0.5m}{\sqrt{l^2 - (\Delta_{21} + 0.5m)^2}}$$

Given that $\Delta_{21}=\mu m$ and substituted in the above equations:

$$\frac{5 - \mu}{\sqrt{n^2 - (5 - \mu)^2}} + \frac{2 - \mu}{\sqrt{n^2 - (2 - \mu)^2}} = \frac{\mu}{\sqrt{n^2 - \mu^2}} + \frac{\mu + 0.5}{\sqrt{n^2 - (\mu + 0.5)^2}} \quad (5-9)$$

among which $n=l/m$.

$$\left. \begin{aligned} \Delta_{11} &= (5 - \mu)m \\ \Delta_{12} &= (2 - \mu)m \\ \Delta_{21} &= \mu m \\ \Delta_{22} &= (0.5 + \mu)m \end{aligned} \right\} \quad (5-10)$$

The equations (5-4) (5-5) (5-9) (5-10) are the calculation formulas of steering characteristics of maglev train with tilting suspension system.

5.2.2 Calculation of steering characteristic parameters of maglev train with tilting suspension system

Structural parameters of vehicle is given, $L=4.096m$; $l=0.24m$; $R=350m \cdot 400m$; gauge is $2.2m$; weight of carriage $W=30T$; $w=W/16=1.875T$. Valuing the convergence accuracy as 0.005 , μ can be obtained by solution of the equation (5-9) with numerical method, then the lateral force f_{ij} and lateral displacement Δ_{ij} of rocker ends derived from equations (5-4) and (5-10), it is not hard to obtain the tension T_{ij} of suspension rocket and the vertical displacement of its ends. The calculation results are as follows:

When the vehicle is passing the curve of $350m$, $R=350m$; $R_1=351.1m$; $R_2=348.9m$.

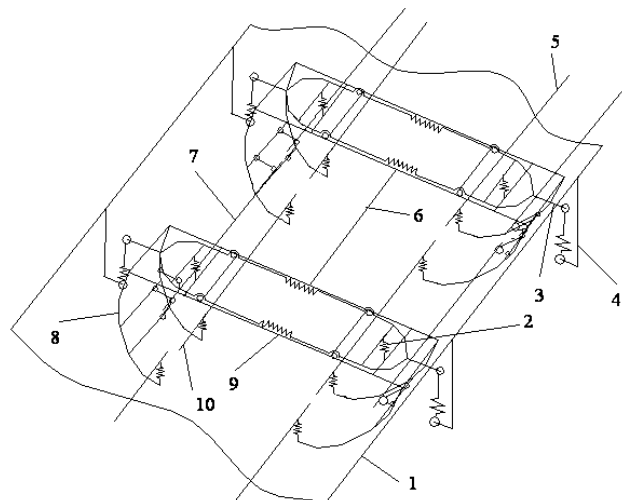
Item Position	Displacement of suspensor rod tip								Lateral force put on car body (KN)			
	Transverse (m)				Vertical (m)				f_{11}	f_{12}	f_{21}	f_{22}
	Δ_{11}	Δ_{12}	Δ_{21}	Δ_{22}	Z_{11}	Z_{12}	Z_{21}	Z_{22}				
Outside track	0.154	0.0106	0.0846	0.1085	0.056	0.0002	0.015	0.026	15.69	0.83	-7.09	-9.54
Inside track	0.156	0.0108	0.0857	0.1098	0.057	0.0002	0.0156	0.027	15.86	0.84	-7.14	-9.37

Table 3. Displacement of suspensor rod tip & Lateral force put on car body

From equation (5-9) it can obtain $\mu=1.777$ and the above parameter table 3. The electromagnetic guiding forces acting on the bogie 1 and 2 are 33.22K and -33.15KN respectively, which is the reason why this kind of vehicles must adopt the active guidance structure.

6. Research on mechanisms and kinematics of maglev bogies

In this paragraph, the mechanism analysis and kinematic calculation methods of maglev bogies are introduced. As described in the paragraph 1 and 2, the bogies of EMS maglev trains have two structures. T-type bogies (Fig.6, 8) are decoupled by the torsion of longerons and A-type bogies (Fig.6, 8) are decoupled by anti-rolling beams. The vertical uncoupling of both kinds of bogies is based on the principle of relative torsion of modules. Their mechanism sketches are shown respectively in Fig.19 and Fig.20.



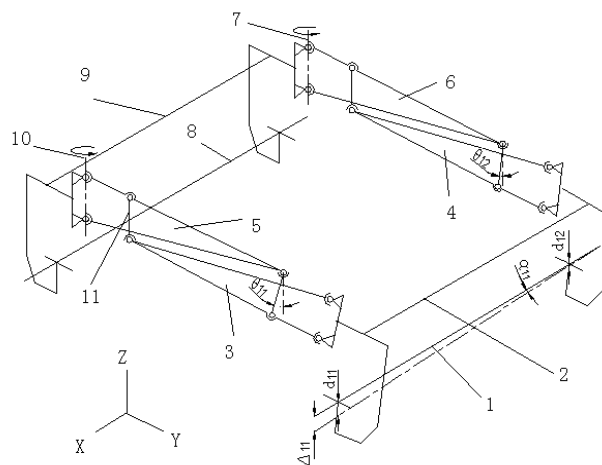
1.Car body, 2.Secondary system spring, 3.Rocker arm, 4.Z support for car body, 5.Linkage levitation magnet, 6.Longeron, 7.Guidance magnet, 8.Support arm, 9.Levitation frame unit, 10.Levitation magnet.

Fig. 20. Mechanism sketch of T-type bogie

The Levitation frame unit of T type bogies is distributed both front and back and may be connected with a torsional elastic longeron, and the Levitation and guidance electromagnet is installed on the bracket arms of front and back modules. It is obvious that other relative motions of the front and back Levitation frame unit of T-type bogies are limited. The two modules of A-type bogie have three translational degrees of freedom and two rotational degrees of freedom. It can be seen from the sketch that the analysis on their X, Y-directional translational degrees of freedom and Z-directional rotational degree of freedom is much simple, and X-directional rotational degree of freedom is limited by the anti-rolling beams, so in this section, the analysis and calculation focus on Z-directional translation and Y-directional rotation of modules of A-type bogies.

Take the kinematic analysis on the right module in Fig. 19 for example. When the endpoint P of right electromagnet 1 elevates D_{11} , the corresponding points M, M' to electromagnets in the same plane with anti-rolling beams 3, 4 elevate d_{11} 、 d_{12} , the angle between the magnet 1 and the horizontal plane is α_1 and the module 2 rotates in the Y direction, namely twist relatively to the left module 9. As the motion of the module 2, the front and back anti-rolling

beams 3, 4 move d_{11} 、 d_{12} upward in the Z direction. Owing to the immovability of the left module 9, as the motion of the module 2, the right and left pairs of anti-rolling beams 3-5,4-6 should stagger d_{11} 、 d_{12} in the Z direction, but the anti-rolling beams are connected by suspenders 1–2 which tend to stop this motion.



1. R. levitation magnet, 2.R. module, 3.R. Front Anti-rolling beam, 4.R.rear Anti-rolling beam, 5.L. Front Anti-rolling beam, 6.L.Rear Anti-rolling, 7.Rear axis of rotation, 8.L. levitation magnet, 9.L. module, 10.Front axis of rotation, 11. Pendular rod

Fig. 21. Module uncoupling movement of a type bogie mechanism

For the sake of further analysis, it may emphasize the analysis on the relative motion of front two anti-rolling beams 3-5. It is obvious that the anti-rolling beam 5 can not move in the Z direction but rotate around the shaft 10. When the module 2 is moving upward, the anti-rolling beam 3 exerts a press force on the Pendular rod 1-1'. Because there are the ball hinges at the ends of the rod, the bearing anti-rolling beam 3 is instability and will deflect to drive the anti-rolling 5 to move around the shaft 10. At this moment, the anti-rolling beam 3 can move upward, namely one end of the module 2 move upward and the other anti-rolling beam moves similarly. It can be seen that the analysis on the motion of modules focuses on the calculation of kinematic parameters of connecting two module ant-rolling beams. The relevant computational formulas are given below.

For the convenience of analysis, the mechanism sketch Fig.21 of ant-rolling beam is given separately. The sketch shows the position relations of motion of all points elevated by one end of the right module. Proposed that the length of ON is L_1 、the length of OP is t_{12} 、the length of OP' is t_{11} 、the length of RM is H_1 、the length of RM' is h_{11} , l_{ij} represents the length of four rocker respectively and the first and second subscripts represent the number of modules and anti-rolling beams respectively.

$$d_{ij} = \frac{t_{ij}}{L_i} \Delta_{ij} \quad i=1, j=1, 2 \quad (6-1)$$

$$\alpha_{ij} = \text{Sin}^{-1} \left(\frac{\Delta_{ij}}{L_i} \right)$$

$$\theta_{ij} = \text{Cos}^{-1} \left(1 - \frac{d_{ij}}{l_{ij}} \right) \quad (6-2)$$

$$S_{ij} = l_{ij} \text{Sin} \theta_{ij} = l_{ij} \sqrt{1 - \text{Cos}^2 \theta_{ij}} \quad (6-3)$$

$$\beta_{ij} = \text{Sin}^{-1} \left(\frac{S_{ij}}{H_i} \right)$$

$$s_{ij} = \frac{h_{ij}}{H_i} S_{ij} \quad (6-4)$$

$$\phi_{ij} = \text{Sin}^{-1} \left(\frac{s_{ij}}{L_{ij}} \right)$$

In above equation (6-3) (6-4), S_{ij} and s_{ij} represent transverse motion of end of pendular rod 1j and 2j respectively, from the above equations :

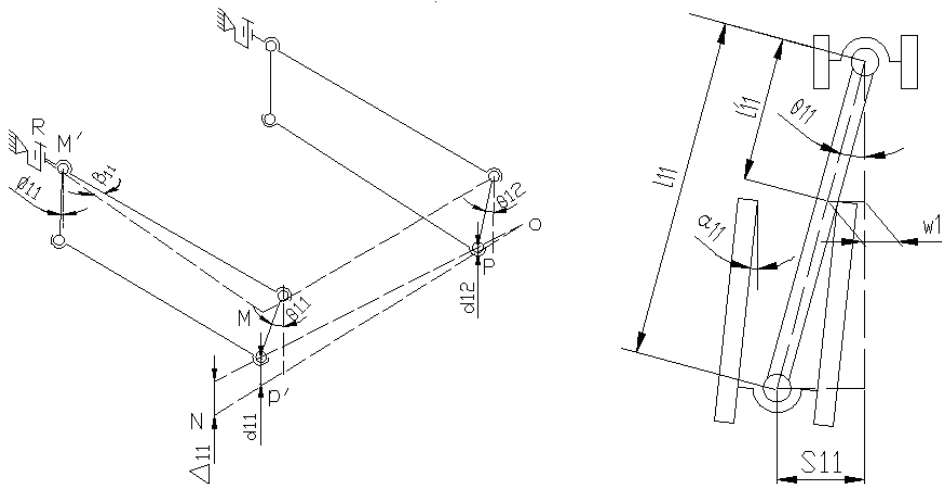


Fig. 22. Z-directional decoupling movement of anti-rolling beam mechanism & oscillation compensation of suspender

$$S_{ij} = l_{ij} \sqrt{1 - \left(1 - \frac{t_{ij} \Delta_{ij}}{L_i l_{ij}} \right)^2} = \frac{t_{ij} \Delta_{ij}}{L_i} \sqrt{\frac{2L_i l_{ij}}{t_{ij} \Delta_{ij}} - 1}$$

$$s_{ij} = \frac{h_{ij} t_{ij} \Delta_{ij}}{H_i L_i} \sqrt{\frac{2l_{ij} L_i}{t_{ij} \Delta_{ij}} - 1}$$

$$\theta_{ij} = \text{Cos}^{-1} \left(1 - \frac{t_{ij}}{L_i l_{ij}} \Delta_{ij} \right)$$

$$\beta_{ij} = \text{Sin}^{-1} \left(\frac{t_{ij}\Delta_{ij}}{L_i} \sqrt{\frac{2L_i l_{ij}}{t_{ij}\Delta_{ij}} - 1} \right)$$

$$\phi_{ij} = \text{Sin}^{-1} \left(\frac{h_{ij}t_{ij}\Delta_{ij}}{H_i L_i l_{ij}} \sqrt{\frac{2l_{ij}L_i}{t_{ij}\Delta_{ij}} - 1} \right)$$

The above equations are the computational formulas of relevant parameters to the Y-directional rotation and Z-directional translation of the right module. When the right module is translating in the Z-direction, $\Delta_{11}=\Delta_{12}$ and the calculation of connecting two pairs of anti-rolling beams is identical. The calculation of X, Y-directional translation and X-directional rotation is comparatively simple and the analysis and calculation of the left module are similar. About these it is unnecessary to go into details.

An example of calculation is given below. Given all relevant geometric dimensions : $ON=L=2700$, $OP'=t_{11}=2320$,

$l_{ij}=200$, $OP=t_{12}=380$, $RM=H_1=1200$, $RM'=h_{ij}=26$ and supposed that one end of module elevates $\Delta_{11}=8\text{mm}$, calculation from the above formula, $S_{11}=52$, $s_{11}=11.3$, $S_{12}=21.2$, $s_{12}=4.6$, $\theta_{11}=15.1^\circ$, $\theta_{12}=6.1^\circ$, $\beta_{11}=2.48^\circ$, $\beta_{12}=1.01^\circ$, $\Phi_{11}=3.24^\circ$, $\Phi_{12}=1.32^\circ$.

If the anti-rolling beams and rocker are assembled as sandwich (Fig.7), the oscillation of pendular rod may be limited, so the width between two anti-rolling beams should be enough. Take the anti-rolling beam 11 for example (Fig.20 right) and it is not difficult to conclude that:

$$w_{11} = \frac{l'_{11}}{l_{11}} S_{11} \quad \text{width between two anti-rolling beams : } W_{11} = \frac{2l'_{11}}{l_{11}} S_{11} + C_{11} , \text{ among which } C_{11}$$

is the diameter of suspender. If $l'_{11} = 75 \text{ mm}$, $C_{11} = 20\text{mm}$, and others are same as the above instance , it is given that $W_{11}=59\text{mm}$.

It should be pointed out that when four rockers are oscillating, connection of four endpoints of the rocker l_{1j} , l_{2j} can form a pair of spatial quadrangles. It has the following two circumstances:

If the module translates in the Z direction, this pair of spatial quadrangles will be in two planes separately and they are parallelogram.

If one end of the module elevates or rotates in the Y direction, this pair of quadrangles will be spatial.

It can be seen that the motion of pendular rod is spatial and the above formulas based on simplified to the plane is approximate one in the circumstance 2. However the error is small and the results are conservative, so there is no problem to apply in the engineering design.

7. Prospects for structure and kinematic analysis on maglev trains

The research and application of maglev trains has gone for more than half century, the study of vehicle structures, focusing on the running gears and secondary suspension system, has

undergone the replacement of many generations. Great strides have also been made in the kinematic analysis which is closely related to design. However, it is to be so regretted that contents of this section is involved in the core of structure and competitiveness and this kind of references are rare, so an brief introduction is given below according to the author's work.

7.1 Prospects for research on vehicle structures

The most feature parts of maglev vehicle structure are the bogies and secondary suspension system for the joint of bogies and car body on which the study touches upon the analysis methods of design and innovation of mechanisms.

1. The research on the mechanism of bogies focuses on the innovation of mechanism which requires providing at most five degrees of freedom for single levitation module. Now the mechanism and its developmental direction are focusing on the spatial linkages mechanism. The number of kinematic pairs and component and joints type are two mainstream research directions, for example, at the longeron's middle of T-type bogie two hinged rods are changed into one rod and more linkage rods are set at the junction part of two modules of A-type bogies. The number of kinematic pairs and component is closely related to degrees of freedom of bogie levitation unit (reduced to connecting rods), and T-type bogies are equipped with more elastic connecting pieces to add the degrees of freedom, which will produce some additional forces and affect their structural life and motion range of component. A-type bogies with plenty of kinematic pairs and component are much complicated in structure and the operation and maintenance work are also increased. Therefore it is an important direction of research on vehicle structure how to constitute the bogie mechanisms with minimum kinematic pairs and components to realize the maximum degrees of freedom now.
2. The innovation of mechanism is still the direction of research on secondary suspension system, but the mechanism of secondary suspension system is closely related to the bogies and is contrary to the bogies in the complexity. This is not hard to understand because the degrees of freedom of bogies are more and the matched secondary suspension system must satisfy its requirements but not limit its degrees of freedom. Therefore an important direction of the research on structure lies in the analysis and innovation of the whole mechanism formed by secondary suspension system and bogies. Of course, the difficulties are obvious.
3. As the advance in the research, the design analysis method is an important branch. It is a trend to apply the development achievements of mechanism in recent years into the structural design of maglev trains. In a nutshell, the topological structure of kinematic chain is represented by graph theory, namely the topological graph represented by points and edges is further represented by matrix. The formulation of experiences and imitation design methods may be very important to the synthesis of bogie mechanism and secondary suspension system. The optimization of mechanisms is another trend, including the objective functions such as scale of motion and degree of freedom and the parameters such as length of linkage rod and connection pair.

7.2 Progress in kinematic analysis on vehicles

The kinematic analysis on vehicles includes kinematic analysis methods, modelling and solutions of kinematics mathematical model, etc.

1. Progress in kinematic analysis methods

At present, the simulation method is widely applied and much mature. The analytic method is still developing and its main direction is to apply the mechanism kinematics theory into the kinematic analysis of maglev trains, for example, in multi-rigid-body kinematical analysis on robots, the traces and relative positions of all rigid bodies can be obtained successively by the determination of the motion trace of input end and D-H transformation, which is method of open chain analysis. However the problem is that the maglev trains have no trace of input end which is conveyed in the fourth section of this chapter, so it is inappropriate to apply the above method into maglev trains. Another analytic method is to found an analytic equation set of the whole kinematic chain by combining geometrical analysis (traces, topological relations among rigid bodies) and equilibrium of internal with external forces, then the equation set is solved to derive traces (instantaneous positions) and topological relations of all bodies (relative positions including the relative positions with traces), which may be called as method of "closed-loop" analysis. That is to say, the traces of the whole kinematic chain and its any component are unknown and all unknown quantities are included in a non-linear equation set. This analytic method is proper to maglev trains and also universal. In this chapter, the analytical process on two kinds of EMS maglev trains introduced.

The further studies include that the dynamics vector equations of vehicles can be obtained by establishing the position vectors equations of spatial traces of all rigid bodies and derivation of the equations on time. In addition, considering the vehicle is composed of rigid-elastic bodies, its method of multi-body kinematic analysis is another important and difficult task.

2. Establishment of kinematics mathematical model

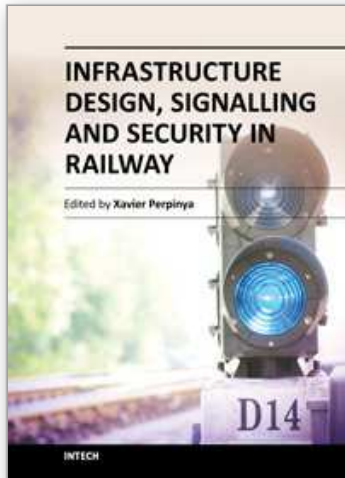
The analytic method is closely related to modelling, Transformation of areal model into space model becomes an important branch even though its sense may be restricted in theoretical category. If the kinematic analysis model of bogies stated in the sixth section is established based on the theory of spatial mechanism, the motion of binding mechanism of modules can be understood clearly and more accurate structural design may be guided if necessary. In addition, the model in the third section can establish the model with the width of vehicle and track by the method of offset curve.

More accurate models are also the pursuit of researchers, for example, considering the influence of change of the module Z-directional displacement caused by the adjustment of electromagnet and elastic elements which may change the kinematic models of maglev trains.

3. The solution should not differ greatly from that of mathematic and numerical solution without much further ado. For maglev trains, their unique features are the simplification of equations, setting of boundary conditions and precision of calculation.

8. References

- Yoshio Hikasa, Yutaka Takeuchi.(1980). Detail and Experimental Results of Ferromagnetic Levitation System of Japan Air Lines HSST-01/=02 Vehicles[C]//IEEE. *IEEE Transactions on Vehicular Technology*, VOL. VT-29, No. 1, February, pp35-41.
- J.L. He, D.M. Rote, and H.T. Coffey (1992). Survey of Foreign Maglev Systems[R]. Center for Transportation Research, Energy Systems Division, Argonne National Laboratory, 9700 South Cass Avenue, Argonne, Illinois 60439, July, pp13-14
- Tejima Yuichi, et al., (2004). Aichi High-speed Traffic HSST-100 Type Vehicle[J]. *Vehicle Technology*, 227(3), pp86-97.
- Seki, Tomohiro.(1995). The Development of HSST-100L[A]. In: *Proceedings MAGLEV'95 14th International Conference on Magnetically Levitated Systems* [C]. VDE-Verlag, ISBN-10 3800721554, Berlin, pp51-55.
- Maglev Technical Committee.(2007). Vehicle Part I General Requirements, In: *Rapid Maglev System Design Principles* [R]. White paper, 12, pp18- 19.
- Z.S.Zhao, L.M.Ying.(2007) One Running Gear of Maglev Vehicle: China, ZL03130750.7[p]. 24. 10.
- Zhao Zhisu, Ren Chao.(2009). Modeling of Kinematics of EMS Maglev Vehicle[J]. *Journal of The China Railway Society*.,Vol.31, (4), pp32-37 · ISSN 1001-8360.
- Zhao Zhi-Su, Et al.,(2000) Motion Analysis and Design for Yawing Mechanism of Maglev Vehicle [J].*Electric Drive for Locomotive*, (6), pp11-13,30, ISSN 1000-128x.
- Mei Zu, Li Jie.(2007). Dynamics Simulation for Yawing Mechanism of Maglev train Based on Virtual Prototype [J]. *Journal of System Simulation*, 19 (18), pp 4199-4203, ISSN 1004-731x
- Jiang Haibo et al.(2007). A Study on Forced Steering Mechanism of Low-speed Maglev Train[J]. *Diesel Locomotive*, (4), pp15-18, ISSN 1003-1839.
- Zeng You-Wen,Wang Shao-Hua.(2003). Research on geometri- cal curve negotiating of three-truck maglev vehicle [J]. *Journal of Southwest Jiaotong University*, 38(3), pp282-285 · ISSN 0258-2724.
- Zhang Kun, LI Jie.(2005). CHANG Wensen. Structure de-coupling analysis of maglev train bogie[J]. *Electric Drive for Locomotive*, (1), pp 22-39, ISSN1000-128x.
- Zhao Chun-Fa, Zai Wan-Ming.(2005). Guidance Mode and dynamic lateral characteristic of low-speed maglev vehicle[J]. *China Railway Science*, (1), pp28-32, ISSN 1001-4632.
- Sinha P. K.(1987). *Electromagnetic Suspension Dynamics & Control* [M]. Perter Peregrinus Ltd., ISBN 10-0863410634, London.
- Luo Kun, Yin Li-Ming, XIE Yun-de.(2004). Analysis on location parameters of line for mid-low speed maglev Train Calculation and analysis of gradient[J]. *Electric Drive for Locomotive*, (4), pp17-19, ISSN 1000-128x.
- Zhao Zhisu.(2009). Researches On Turing Characteristic Of Tilting Suspension High-Speed Maglev Train[J]. *Electric Drive for Locomotive*, (1), pp43-45, ISSN 1000-128x.



Infrastructure Design, Signalling and Security in Railway

Edited by Dr. Xavier Perpinya

ISBN 978-953-51-0448-3

Hard cover, 522 pages

Publisher InTech

Published online 04, April, 2012

Published in print edition April, 2012

Railway transportation has become one of the main technological advances of our society. Since the first railway used to carry coal from a mine in Shropshire (England, 1600), a lot of efforts have been made to improve this transportation concept. One of its milestones was the invention and development of the steam locomotive, but commercial rail travels became practical two hundred years later. From these first attempts, railway infrastructures, signalling and security have evolved and become more complex than those performed in its earlier stages. This book will provide readers a comprehensive technical guide, covering these topics and presenting a brief overview of selected railway systems in the world. The objective of the book is to serve as a valuable reference for students, educators, scientists, faculty members, researchers, and engineers.

How to reference

In order to correctly reference this scholarly work, feel free to copy and paste the following:

Zhao Zhisu (2012). Structural and Kinematic Analysis of EMS Maglev Trains, Infrastructure Design, Signalling and Security in Railway, Dr. Xavier Perpinya (Ed.), ISBN: 978-953-51-0448-3, InTech, Available from: <http://www.intechopen.com/books/infrastructure-design-signalling-and-security-in-railway/maglev-train-and-its-kinematics-analysis>

INTECH
open science | open minds

InTech Europe

University Campus STeP Ri
Slavka Krautzeka 83/A
51000 Rijeka, Croatia
Phone: +385 (51) 770 447
Fax: +385 (51) 686 166
www.intechopen.com

InTech China

Unit 405, Office Block, Hotel Equatorial Shanghai
No.65, Yan An Road (West), Shanghai, 200040, China
中国上海市延安西路65号上海国际贵都大饭店办公楼405单元
Phone: +86-21-62489820
Fax: +86-21-62489821

© 2012 The Author(s). Licensee IntechOpen. This is an open access article distributed under the terms of the [Creative Commons Attribution 3.0 License](#), which permits unrestricted use, distribution, and reproduction in any medium, provided the original work is properly cited.

IntechOpen

IntechOpen